Research Article

Song Gao#, Jianlin Luo*#, Jigang Zhang, Fei Teng, Chao Liu, Chao Feng, and Qian Yuan

Preparation and piezoresistivity of carbon nanotube-coated sand reinforced cement mortar

https://doi.org/10.1515/ntrev-2020-0112
received November 30, 2020; accepted December 19, 2020

Abstract: Water and sand were used as the medium of multiwall carbon nanotube (MCNT) and prepared MCNT aqueous suspension and MCNT suspension-coated sand, respectively; afterwards, they were introduced into cement mortar (MNT/CM, MNTSM), respectively. Next, mechanical strengths and piezoresistive properties (DC resistivities (ρ_v), AC impedances (Z_r)) under cyclic loadings (σ_c) of two types of MNT/CM and MNTSM nanocomposites were investigated to explore the intrinsic and self-sensing behaviors. Results reveal that MCNT can be evenly and well-coated on sand, which favors to achieve its intrinsic self-sensing property. Although the fraction changes in ρ_v and Z_r under the same σ_c of MNTSM are both lower than those of MNT/CM, the stress sensitivity of MNTSM is only −1.16%/MPa (DC resistivity), −1.55%/MPa (AC impedance); its sensing linearity and stability (2.53, 2.45%; 2.73, 2.67%) are superior to those of MNT/CM (4.94, 2.57%; 3.78, 2.96%). Piezoresistivity using AC impedance technique is helpful to acquire balanced sensing sensitivity and stability while applied as intrinsic sensors in infrastructure.

Keywords: carbon nanotube, dispersion method, CNT-coated sand, AC impedance, piezoresistive property

1 Introduction

It's crucial to prevent from possible structure failure and guarantee in-serve safety of concrete structures using a variety of sensors, just like visual detectors, optical fibers, piezoelectric ceramics, electromagnetic transducers, and cement-based sensors. Considerable attention on intrinsic sensors has been paid in last several decades. Lee *et al*. designed and fabricated wireless cement-based sensors and signal transmission module for self-monitoring of railway concrete infrastructures with similar sensing response and gauge factor [1]. Chung reviewed carbon materials for significant emerging applications that relate to structural self-sensing, electromagnetic interference shielding, and thermal interfacing [2]. Luo *et al*. developed a 0–3 type PZT/chrysotile fiber/cement composite intrinsic piezoelectric sensor with balanced sensing responses and toughness for self-monitoring [3].

Cement-based sensors-related researches exhibit application prospect owing to their easy preparation, low cost, long durability, and good impedance compatibility to concrete structures. Meanwhile, electrical signals are sensitive to dielectric concrete when suffering chloride ion, sulfate, carbon dioxide, other electrolyte invasions, etc. Al-Dahawi *et al*. assessed self-sensing performances by AC impedance under varied frequencies [4]. Sanchez *et al*. used on-site resistivity to evaluate durability of reinforced concrete [5]. Danoglidis *et al*. used electrochemical impedance spectroscopy to quantitatively study the impact of CNT content in nanoreinforced cement [6]. Reiterman *et al*. used resistivity change to characterize freeze-thaw resistance of cement screed [7]. In fact, as a noninvasive methodology, electrical signals are often employed to evaluate the status of conducting cement-based sensor

# These authors contributed equally to this work.

*** Corresponding author: Jianlin Luo,** Department of Materials Science and Technology, School of Civil Engineering, Qingdao University of Technology, Qingdao, 266525, China; Collaborative Innovation Center of Engineering Construction and Safety in Shandong Blue Economic Zone, Qingdao, 266525, China, e-mail: lawjanelim2009hit@gmail.com, lawjanelim@qut.edu.cn, tel: +86-532-85071605, fax: +86-532-85071605
Song Gao, Jigang Zhang: Department of Materials Science and Technology, School of Civil Engineering, Qingdao University of Technology, Qingdao, 266525, China; Collaborative Innovation Center of Engineering Construction and Safety in Shandong Blue Economic Zone, Qingdao, 266525, China
Fei Teng, Chao Feng, Qian Yuan: Department of Materials Science and Technology, School of Civil Engineering, Qingdao University of Technology, Qingdao, 266525, China
Chao Liu: School of Civil Engineering, Qingdao University of Technology, Qingdao, 266525, China; Jiangsu Key Laboratory of Construction Materials, School of Materials Science and Engineering, Southeast University, Nanjing, 211189, China

filled with some conductive admixtures, such as steel fiber, carbon fiber (CF), nickel powder, carbon black, carbon nanotube (CNT), carbon nanofiber, conductive graphene flake, etc., when embedded in structure and suffering external load or deformation. Li *et al.* employed electrical resistivity to evaluate compressive strain change of carbon black-filled cement-based composite [8]. Luo *et al.* evaluated the effect of MCNT fraction, moisture, and stress/strain level on electrical properties of MCNT cement-based composite [9]. Ventrapragada *et al.* used electric capacity to test CNT-coated paper as current collectors [10].

CNT possesses superior mechanical properties in tandem with conductivity compared with conventional conductive fillers, as documented by Power *et al.* [11] and Lin *et al.* [12]. Considerable researchers have focused on CNT cement-based sensors and developed them as embedded sensors used in traffic monitoring, frequencies identification, strain and deformation sensing, and cracking prewarning. Zhan *et al.* synthesized carbon nanotubes (CNTs) in situ on the surface of fly ash to improve the dispersibility of CNTs and obtained outstanding strain sensing capability of intrinsic CNT/mortar sensors [13]. Han *et al.* launched nano-carbon-engineered cementitious composites with self-sensing, self-damping, self-repairing multifunctions [14], developed a self-sensing CNT/cement sensor for traffic monitoring [15], and integrated a self-sensing CNT concrete pavement system for traffic detection [16]. Dong *et al.* investigated piezoresistivity of a CNT/cement sensor while exposed to elevated temperatures [17]. Li *et al.* launched piezoresistivity of a CNT/cement composite after oxidized functionalization to CNT [18]. D'Alessandro *et al.* developed a scalable fabrication procedure for self-sensing CNT/cement sensors for SHM [19].

It is still a challenge to fully disperse CNT in aqueous cement/concrete matrix, which severely limits CNT-wide applications in construction industry. Luo *et al.* studied five surfactants on the dispersion of CNT in water, cement aiding with sonication [20], and employed Fenton/UV oxidation on CNT to enhance its dispersivity [21]. Isfahani *et al.* [22] used UV-vis spectroscopy to evaluate the dispersivity of CNT. Collins *et al.* [23] argued the admixtures of air entrainer, styrene butadiene rubber, polycarboxylates, calcium naphthalene sulfonate, and lignosulfonate on the dispersion of CNT through workability testing of selected OPC-CNT-dispersant/surfactant paste. Hu *et al.* [24] used humic acid to assist stabilization of dispersed CNT. Gao *et al.* evaluated ultrasonication energy input on the dispersion of CNT [25] and nanoreinforcement of graphene oxide-CNT [26]. Kim *et al.* used fly ash [27] and silica fume [28] to enhance the CNT dispersion in water and cement matrix with low water-binder ratio. Roy *et al.* [29] and Hanizam *et al.* [30] employed similar method to obtain good dispersion of CNT in polymer and metal matrix, respectively.

Some scholars further improved sensing capacity, sensitivity, and linear repeatability of CNT/cement composite sensors using hybrid conductive fillers along with CNT. Azhari *et al.* [31] reported better repeatability combined with CFs and CNTs in cement. Panagiota *et al.* [32] found timely failure warnings and strain sensing potentials hybrid with carbon nanofibers and CNTs in cement. Lee *et al.* [33] documented good piezoresistive properties of cement composite hybrid with CFs and CNTs. Han *et al.* [34] reported self-sensing smart behavior of cement botryoid hybrid nano-carbon materials. Yoo *et al.* [35] documented peizoresistive gauge factor of 166.6 for hybrid CNTs in cement. Luo *et al.* [36] reported more stable repeatability on piezoresistive behavior of hybrid fillers-modified cement composite than that of with single fillers.

It's worth noting that the Young's modulus of cement paste without aggregate backbone is below than that of the corresponding mortar or concrete, and the shrinkage cracking of the former is also apt to happen. Metaxa *et al.* [37] documented substantial improvement of the mechanical properties after use of effectively dispersed MWCNT/aqueous/surfactant suspensions in cement. Song *et al.* [38] found that well-dispersed CNTs increased compressive strength and modulus of elasticity and decreased autogenous shrinkage of cement mortar. Stynoski *et al.* [39] documented substantial improvement of fracture and mechanical properties of cement reinforced with CF and CNT. Notwithstanding, superior strengthening and crack bridging effect of CNT favor the corresponding CNT-based cement sensor with a little resultant higher modulus and mechanical strength with respect to the plain cement paste.

These inevitably impair the modulus matching and compatibility of deformation between embedded cement-based sensor and concrete structure. It's urgent to develop mortar, even concrete-based sensor with aggregate backbone. Modest literatures have reported on the preparation and performance of CNT mortar or concrete-based composites [38–44]. Kostrzanowska-Siedlarz *et al.* [40] used a Bingham model to describe the rheological properties of CNT/mortar. Geraldo *et al.* [41] concepted a simple and economically viable way of incorporating CNT at building sites with resultant improvements in mechanical properties of mortar. Metaxa *et al.* [42] designed metallic "I"-shaped connectors casting CNT reinforced mortar as a sensor to monitor the structural integrity of restored marble epistyles under shear. Hawreen *et al.* [43] argued that shrinkage and fracture toughness, compression,

flexion, and elastic modulus of mortars highly improved with CNT incorporation and found CNTs provided efficient crack bridging and enhanced quality of aggregate-paste ITZ. Kaur *et al.* [44] reported improved mechanical strength of mortar dosing with graphene oxide and CNT. Yet, the researches related to the piezoresistive behavior of CNT mortar-based sensor are seldom found.

In the present work, we employed water and sand as the medium of CNT and prepared CNT aqueous suspension and CNT-coated sand, allowing both to be the ingredients of mortar, respectively; afterwards, they were introduced into cement mortar pre-inserted with a pair of electrodes along the longitude. Next, we focused on mechanical and piezoresistive properties (DC resistivity, AC impedance) of two types of mortars under cyclic compressive loading [45], which favors to develop high-performance intrinsic sensors applied in concrete structures.

2 Materials and experimental details

2.1 Raw materials

The cement, ordinary Portland cement (P.O.42.5 type), was obtained from Shanshui Cement Inc. (Qingdao, China). Sand, granite mountain sand with 2.1 fineness modulus and even gradation, was locally commercially available; Table 1 lists its chemical composition and physicochemical properties, and Table 2 presents the corresponding physical performances, which are in line with requirements of GB/T07671-1999 standard (China). Superplasticizer, polycarboxylate ester-based high range water-reducer (PCE, PCA-I type), was acquired from Jiangsu Sobute New Material Co. Ltd (Nanjing, China); Water, tap water was available.

Multiwall carbon nanotube (MCNT), in CVD process, was purchased from Chengdu Institute of Organic Chemistry, Chinese Academy of Sciences (Chengdu, China); the main physical properties of MCNT are also shown as Table 2. *N*-Methyl-2-pyrrolidone (NMP, AR) and sodium dodecyl benzene sulfonate (SDBS, AR), serving as the solvent, MCNT's dispersant, were both purchased from Shanghai Ebi Chemical Reagent Co., Ltd (Shanghai, China). Triton X-100 (TX10, OP), serving as the emulsifier of MCNT, was purchased from Sinopharm Group Chemical Reagent Co., Ltd (Shanghai, China). Styrene-acrylic latex (SA), serving as MCNT suspension thickener and interface adhesive with sand, was purchased from Shanghai Tiandi Coating Co. Ltd (Shanghai, China).

2.2 Preparation of MCNT aqueous dispersion and MCNT-coated sand

Figure 1 presents the preparation procedure of MCNT-coated sand; the details were shown as in the following. First, SDBS: TX10: NMP was mixed in mass ratio of 2:1:95 with a magnetic stirrer (JY85-1 type, Jintan, China), SA, MCNT was added into the above solution in 20, 2 wt% dosage, respectively. Second, MCNT/SA suspension was prepared with employing a dispersing homogenizer (FJ200-SH type, Shanghai, China) for 15 min at 2,000 rpm, subsequently ultrasonicating for 1.5 h at 100 W, 40 kHz in a bath sonicator (KH2200DB type, Changzhou, China) in tandem

Table 1: Main physicochemical properties of ordinary Portland cement and granite mountain sand

Type	Chemical composition (wt%)							
	SiO_2	Al_2O_3	CaO	Fe_2O_3	SO_3	K_2O	Na_2O	LOI
P.O. 42.5 cement	21.2	63.1	5.9	2.9	3.3	0.65	0.11	0.77
Granite sand	67.5	17.6	4.8	3.4	—	0.1	0.37	1.6

Type	Physicochemical index								
	Density (g/cm^3)	BET surface (kg/m^2)	Soundness	Setting time (min)		Flexural strength (MPa)		Compressive strength (MPa)	
				Initial	Final	3 days	28 days	3 days	28 days
P.O. 42.5 cement	3.10	356.0	Qualified	175	255	3.5	6.0	17.9	42.5

Table 2: Main physical properties of granite mountain sand and MCNT

Granite sand	Dried compressive strength (MPa)	Saturated compressive strength (MPa)	Apparent density (kg/m³)	Bulk density (kg/m³)	Void ratio (kg/m³)	Elastic modulus (GPa)	Degree of fineness
	144.2	139.9	2,622	1,517	42.1	1.3	2.1
MCNT	**Production proocess**	**Outer diameter (D/nm)**	**Length (L/μm)**	**Mass purity (wt%)**	**BET surface area (m²/g)**	**Electrical conductivity (S/cm)**	**Density (g/cm³)**
	CVD	10–20	10–15	≥95	≥165	≥100	1.6

with recycling cooling water. Third, 3 kg granite sand after oven-dry was divided into three batches and fully spread out till the thickness of each batch was around 6 mm. Fourth, 150 mL MCNT/SA suspension was in-batch sprayed onto the spread-out sand layer at 40 cm distance by a sprayer (W71 type, Taizhou, China); after surface drying, the sprayed sand layer was flipped over by a plastic spade for spraying process on the other side of the sand. Fifth, four-round spraying with pipeline procedure was treated for each spread-out sand layer; the MCNT-coated sand was ventilated-dried and then oven-dried in a vacuum oven (DZF-6210 type, Shanghai, China) at 55 ± 1°C for 30 min. The schematic flowchart is demonstrated in Figure 1. It's worth noting that some sample of MCNT-coated sand was incinerated with a high-temperature furnace (SX2-16-10 type, Longkou, China) with the resultant 19.2 wt% organic content.

The cement slurry was blended in water/cement ratio (W/C) of 0.4, superplasticizer fraction (w_{PCE}) of 1 wt%, and the MCNT-coated sand was mixed into cement slurry with cement to MCNT-coated sand ratio of 1:2.192 for 240 s to prepare MCNT-coated sand-modified cement mortar (MNTSM) according to the GB/T07671-1999 standard (Beijing, China). MCNT/SA suspension in 19.2 wt% of normal sand content was directly mixed into normal cement mortar with the same W/C, w_{PCE}, and cement/normal sand ratio of 1:2 to prepare normal MCNT-modified cement mortar (MNT/CM). Meanwhile, the plain cement mortar without any MCNT (CO) was also prepared with the same W/C, w_{PCE} of 1 wt%, w_{SA} of 20 wt%, and cement/normal sand ratio of 1:2 according to GB/T07671-1999 standard (Beijing, China). After vibration compaction via a vibrating compact table (ZS-15 type, Wuxi, China), the well-blend slurry of each group mortar was poured into six oiled prism molds in size of 160 × 40 × 40 mm. Three of them in each group were with pre-inserted pair of in-parallel copper electrodes at 60 mm intervals, and the other three were without electrodes. All mortar specimens were cured to 28 days in a standard curing room in 22 ± 3°C temperature and >95% R.H. condition.

2.3 Characterization of physical properties

The naked, optical morphology of MCNT-coated sand after oven-dry was acquired with a digital camera (Canon EOS3 type, Shanghai, China) and an optical microscopy (XC4 type, Shanghai, China), respectively [46]. The 28 days-cured flexural strength (f_b^{28}) of three

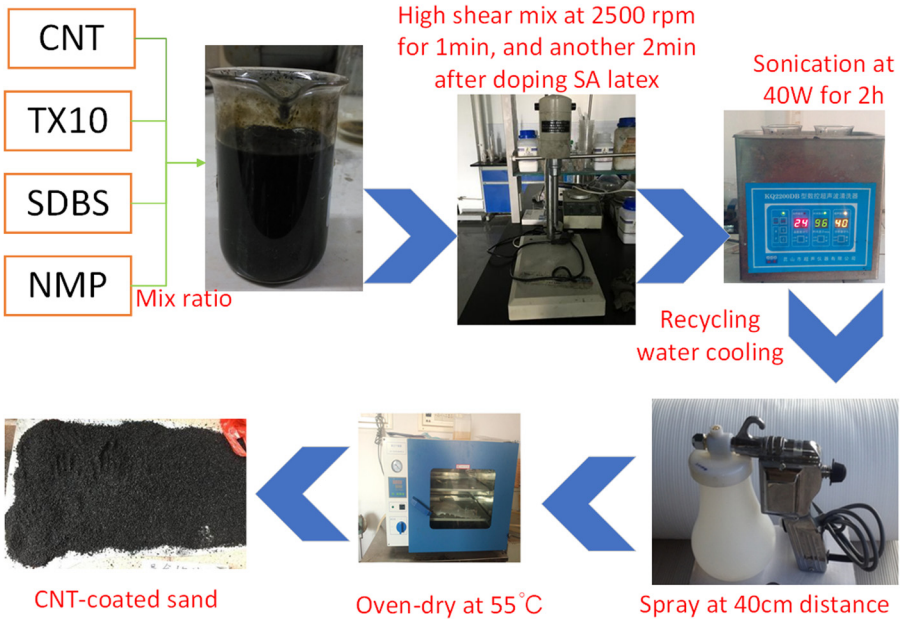

Figure 1: The schematic procedure of MCNT coating onto sand.

types of cured mortar specimens (MNT/CM, MNTSM, CO) was characterized by a universal material testing machine (DY-208M type, Wuxi, China) at 0.05 MPa/s cross-head speed, and the compressive strength (f_c^{28}) of six half-split duplicates was accordingly characterized at 0.5 MPa/s cross-head speed in line with GB/T17671-1999 standard (Beijing, China).

As for piezoresistivity test for the other three specimens in the same group, a universal material testing machine (CMT5205/5305 type, MTS Industrial Systems (China) Co., Ltd, Jinan, China) was used to apply cyclic loading/unloading onto the erect specimen in triangle wave mode from 0 to 6 MPa at 50 N/s cross-head speed. Meantime, a digital multimeter (VC890c type, Shenzhen, China), digital LCR bridge (TH2817B type, Tonghui, China), measured the electrical volume resistances (R_vs), the real part of AC impedances at 100 kHz frequency (Z_rs) of the specimen, respectively [45]. The configuration of the DC/AC piezoresistive testing is demonstrated in Figure 2a and b. The corresponding resistivities (ρ_vs) can be achieved by the equation $\rho_v = R_vS/L$; here S and L are the contact cross-area and interval distance of the electrodes, respectively [36].

Some tiny samples of the MNTSM and MNT/CM after mechanical crushing were oven-dried in a vacuum oven (DZF-6210 type, Shanghai, China) at 55 ± 1°C for 48 h; hereafter, scanning electronic microscopy (SEM, Helios NanoLab 600 type, USA) was employed to observe the corresponding microstructures after top surface Au-sprayed.

3 Results and discussion

3.1 Dispersion effectiveness of MCNT in mortar

The naked and optical photos of oven-dry MCNT-coated sand are shown in Figure 3.

As revealed in Figure 3a, MCNT is evenly and well-coated on sand, aiding with SA latex and high shear dispersion method, which favors to good bonding effect between MCNT and sand [41]. Figure 3b and c demonstrate that although overwhelming majority of MCNT/SA latex is deposited on the island-like surfaces of sand, and mutual connected, some trace of MCNT/SA latex is still deposited in the middle of the sand surface and isolated with the rest. The initial ρ_v of MNT/CM, MNTSM, and CO group is 20, 45, and 990 kΩ cm, respectively, which implies the dispersivity effect of conductive MCNT in MNT/CM is superior to that in MNTSM, also verified by SEM microstructure in Figure 4. Most of CNT was individually dispersed in MCNT/CM other than rarely local agglomeration found, as presented in Figure 4a and c.

Figure 2: The piezoresistive test configuration of MNTSM or MNT/CM with two-electrode method: (a) DC resistance (yellow box – MNTSM or MNT/CM specimen with two electrodes); (b) AC impedance.

However, most of CNT was in local agglomerating state and scattered in MNTSM other than few dotted-like individual CNT nanofibers crossing micro-cracks, as shown in Figure 4b and d [47].

3.2 Mechanical properties of MNT/CM and MNTSM

As revealed in Figure 5, the f_b^{28}s and f_c^{28}s of MNTSM, MNT/CM groups are both higher than those of CO group, but the corresponding deviations are a little higher than those of CO group. The maximum amplitudes of f_b^{28} and f_c^{28} of MNTSM, MNT/CM climb up to 6.6, 13.0%; 15.2, 14.2% with respect to those of CO, respectively. These imply that MCNT incorporation with superior pulling-out effect is positive to the enhancement of mechanical strengths (f_b^{28}s and f_c^{28}s) of the mortar, either one-step direct incorporation or two-step incorporation with firstly coated on the sand method, which is similar to ref. [23] claimed.

It's worth noting that the f_b^{28}s and f_c^{28}s of MNTSM are both slightly lower than those of MNT/CM, esp. f_c^{28}s,

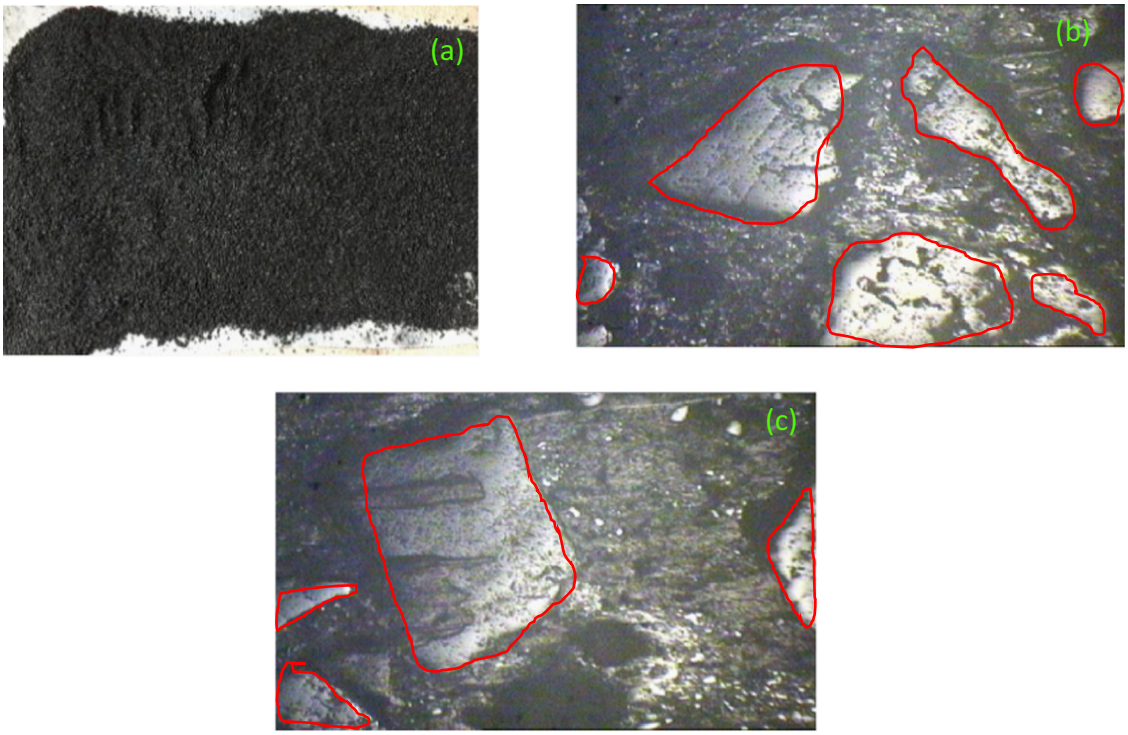

Figure 3: Photos of MCNT-coated sand in: (a) naked scale; (b) and (c) optical scale (×200 magnification) (red polygons – island-like sand surface surrounded with CNT/SA latex).

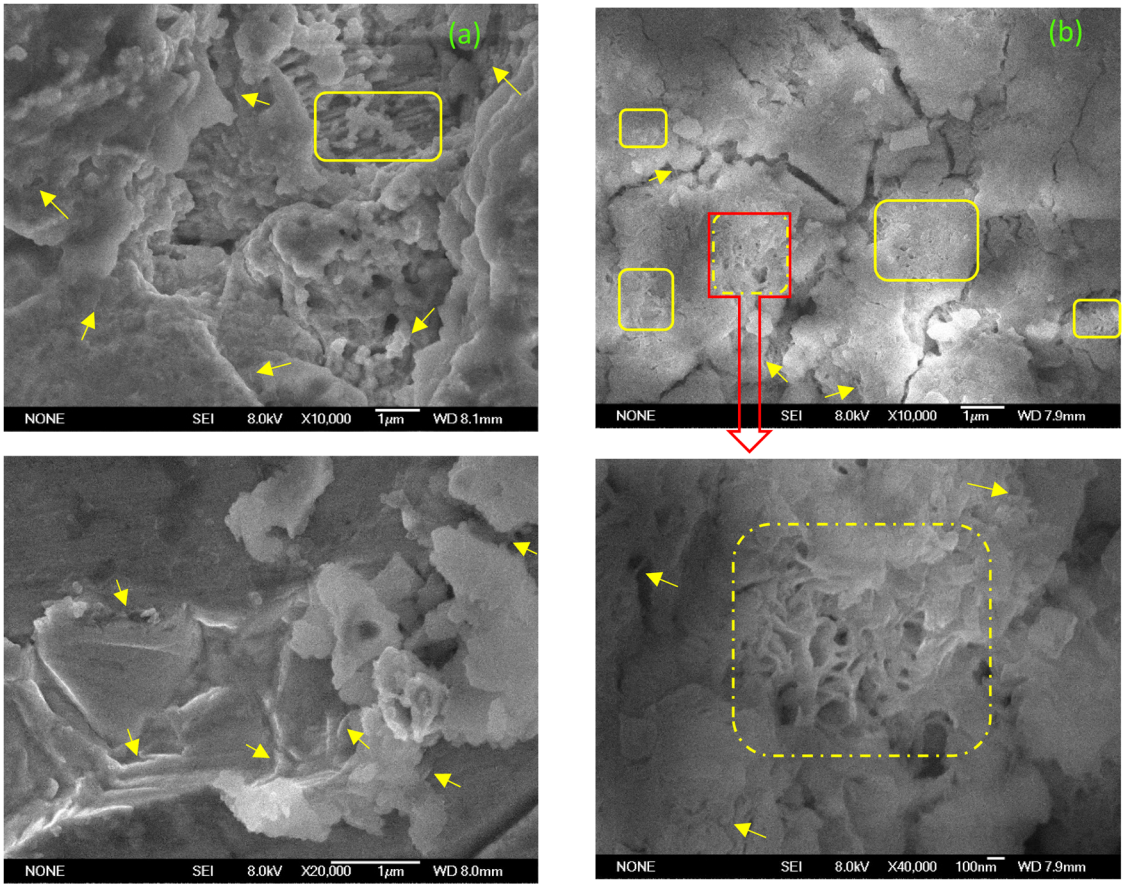

Figure 4: SEM images: (a) MCNT/CM; zoomed with 10k, 20k (top-left, bottom-left); (b) MNTSM zoomed with 10k, local enlargement red box of top-right image (top-right, top-bottom) (arrow-single CNT; rounded rectangle – CNT agglomerations).

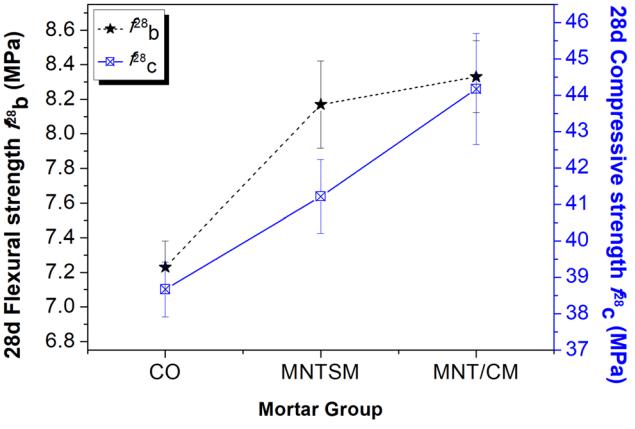

Figure 5: The flexural and compressive strengths of MNTSM, MNT/CM, and CO.

which indicates that the hydration texture and density of MNTSM with two-step incorporation method are somewhat inferior to those of MNT/CM with one-step method under sufficient dispersion condition, as revealed in Figure 4. In one hand, some connected fractures and cracks exist in the microstructure of MNTSM, rendering discontinuity of cement hydrations as also can be verified by Figure 4b; in other hand, some MCNT is in local agglomerating state and loose textures are found in the interface between MCNT-coated sand and cement hydration; both are harmful to the final macroscale strength, as demonstrated in Figure 4b. In fact, dense textures and interlocking between cement hydration and coated sand of MNTSM can be achieved by proper dispersants and latex emulsifier selection, as verified in Figure 4b, as also documented in ref. [41].

3.3 Piezoresistive properties of MNTSM and MNT/CM

As there is almost no regular change in ρ_v or Z_r under cyclic loading for CO group, here we just focused on the corresponding fraction changes in ρ_v ($\Delta\rho_v$) or Z_r (ΔZ_r) of

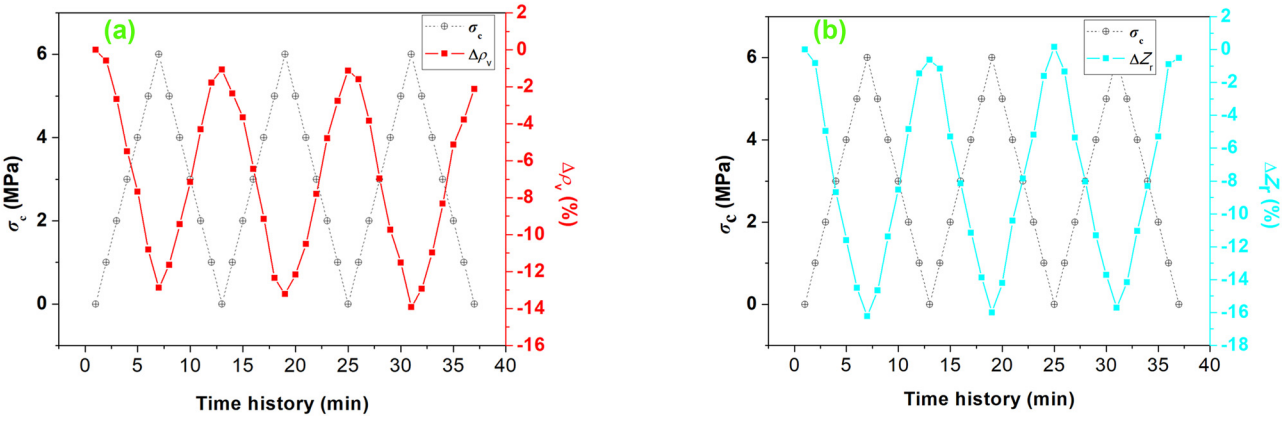

Figure 6: The piezoresistive curves of MNT/CM: (a) $\Delta\rho_v - \sigma_c$ relation; (b) $\Delta Z_r - \sigma_c$ relation.

MNT/CM, MNTSM under cyclic loading (σ_c), as presented in Figures 6 and 7, respectively. And the corresponding sensitivity (S_ρ, S_Z), linearity (l_ρ, l_Z), repeatable stability (r_ρ, r_Z) of the $\Delta\rho_v - \sigma_c$, and $\Delta Z_r - \sigma_c$ curves of MNT/CM and MNTSM can be deduced from the sensor parameters formula – Equations (1–3) – details presented in Table 3.

$$S_{\rho,Z} = (\Delta\rho_v/\rho_v)/\sigma_c \text{ or } (\Delta Z_r/Z_r)/\sigma_c \tag{1}$$

$$l_{\rho,Z} = \pm\Delta_{max}/(\Delta\rho_v/\rho_v)F \cdot S \times 100\% \text{ or } \pm\Delta_{max}/(\Delta Z_r/Z_r)F \cdot S \times 100\% \tag{2}$$

$$r_{\rho,Z} = \pm\Delta_{max}\,1/(2\Delta\rho_v/\rho_v) \times 100\% \text{ or } \pm\Delta_{max}\,1/(2\Delta Z_r/Z_r) \times 100\% \tag{3}$$

where: $\Delta\rho_v/\rho_v$, $\Delta Z_r/Z_r$ is the fraction change rate in volume resistivity ($\Delta\rho_v$), impedance (ΔZ_r) vs initial ρ_v, Z_r, respectively; σ_c is the subjected compressive stress (MPa); Δ_{max}, $(\Delta\rho_v/\rho_v)_{F.S}$, $(\Delta Z_r/Z_r)_{F.S}$ represents the maximum deviation between the $\Delta\rho_v$–σ_c, ΔZ_r–σ_c curve and the linear fitting line and the full-scale output of $(\Delta\rho_v/\rho_v)$, $(\Delta Z_r/Z_r)$, respectively; $\Delta_{max}1$ represents the maximum output non-repetitive error.

As shown in Figures 6 and 7 and Table 3, in general, the maximal ΔZ_r of MNT/CM can reach –16.22% when the σ_c is at 6 MPa; the corresponding S_ρ, S_Z of MNTSM (–1.16, –1.55%/MPa) are both lower than those of MNT/CM (–2.15, –2.7%/MPa), respectively; details are shown in Table 3. It's worth noting that MCNT nanofibers with one-step dispersion method can achieve more sufficient distribution and more conducting pathways formation than nanotubes with sand-coated two-step method within mortar matrix, also verified by the initial ρ_v and microstructure demonstrated in Figure 4.

But these sensitivities (S_ρ, S_Z) are all advantageously higher than the bulk cement-based pressure-sensitive sensor, which renders MNT/CM or MNTSM to be a good candidate among intrinsic sensor attached for concrete monitoring [36]. It's worth to point out that the linearity (l_ρ, l_Z) and repeatable stability (r_ρ, r_Z) of MNTSM (2.53, 2.45%; 2.73, 2.67%) are all superior to those of MNT/CM

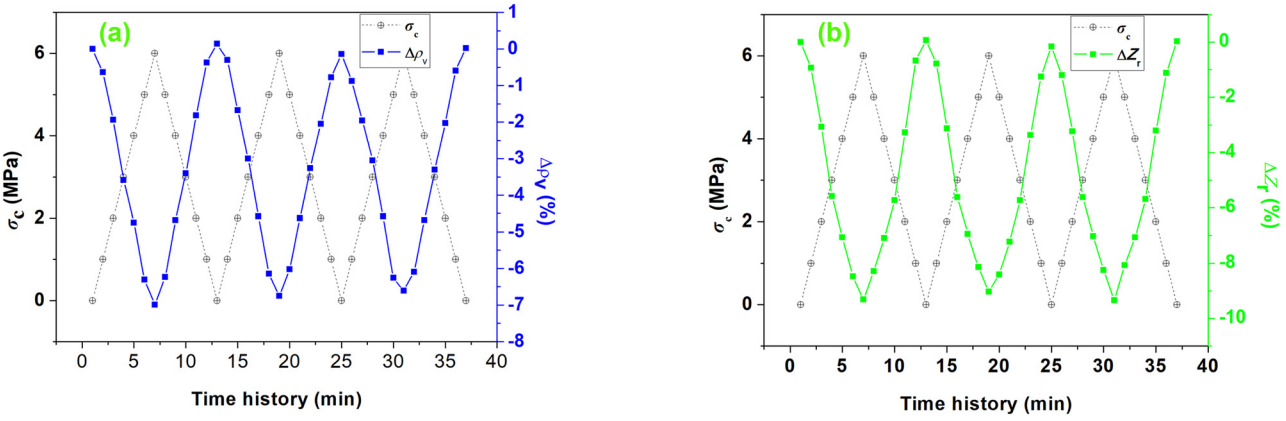

Figure 7: The piezoresistive curves of MNTSM: (a) $\Delta\rho_v - \sigma_c$ relation; (b) $\Delta Z_r - \sigma_c$ relation.

Table 3: Piezoresistive sensing parameters of MNT/CM and MNTSM

Specimen no.	S_ρ (%/MPa)	S_Z (%/MPa)	l_ρ (%)	l_Z (%)	r_ρ (%)	r_Z (%)
MNT/CM	−2.15	−2.70	4.94	2.57	3.78	2.96
MNTSM	−1.16	−1.55	2.53	2.45	2.73	2.67

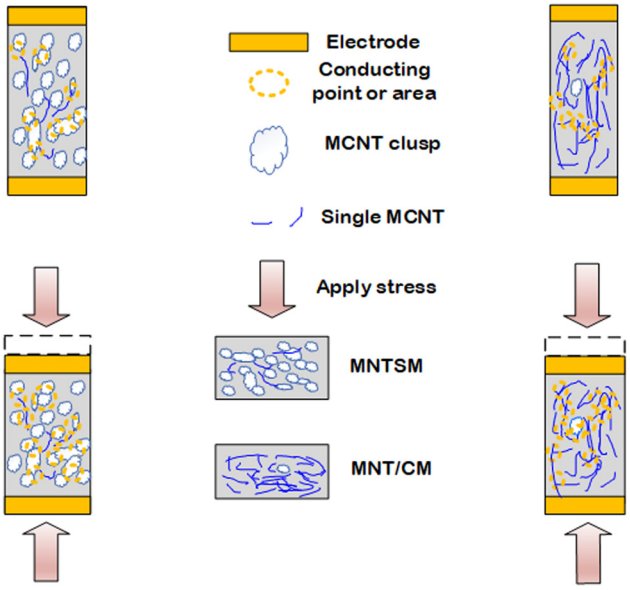

Figure 8: The conducting mechanism of MNTSM, MNT/CM under compressive loading.

(4.94, 2.57%; 3.78, 2.96%). In fact, despite more conducting pathways formation for MNT/CM than MNTSM, the conducting pathways owing to overlapping and contact points or areas of MCNT coating layer on the sand in MNTSM are more tough and robust than the single nanofiber connecting or closing points or areas within MNT/CM, as schematic shown in Figure 8. These less but robust pathways contribute to better linearity and stability for MNTSM than MNT/CM, which is more advantageous when subjected to cyclic loading [27].

4 Conclusions

In this study, water and sand were employed as the medium of MCNT dispersion into cement mortar and mechanical, electrical, and piezoresistive properties of two types of MCNT-modified cement mortar were investigated. Some conclusions are drawn as follows:

(1) MCNT can be evenly and well-coated on sand aiding with SA coating and high shear dispersion method.
(2) The f_b^{28}s and f_c^{28}s of MNTSM and MNT/CM climb up to 6.6, 13.0%; 15.2, 14.2% with respect to those of CO owing to the fiber bridging effect exertion of MCNT.
(3) The $\Delta\rho_v$ and ΔZ_r under the same σ_c of MNTSM (−1.16, −1.55%/MPa) are both lower than those of MNT/CM, but the sensing linearity (2.53, 2.45%) and stability (2.73, 2.67%) of MNTSM are superior to those of MNT/CM.
(4) Piezoresistivity using AC impedance method favors to acquire balanced sensing sensitivity and stability for either MNT/CM or MNTSM when applied as intrinsic sensors in infrastructure.

Acknowledgments: The work has been financially supported by the NSFC-Shandong Province Joint Key Project (Grant No. U2006223), National Natural Science Foundation of China (Grant No. 51878364 and 51978353), Natural Science Foundation of Shandong Province (Grant No. ZR2018MEE043), Key Technology Research and Development Program of Shandong Province (Public welfare type) (Grant No. 2019GSF110008), the National “111” project, and first-class discipline project funded by the Education Department of Shandong Province.

Conflict of interest: The authors declare no conflict of interest regarding the publication of this paper.

References

[1] Lee SJ, Ahn D, You I, Yoo DY, Kang YS. Wireless cement-based sensor for self-monitoring of railway concrete infrastructures. Autom Constr. 2020;119:103323–32.
[2] Chung DDL. Carbon materials for structural self-sensing, electromagnetic shielding and thermal interfacing. Carbon. 2012;50:3342–53.
[3] Luo JL, Zhang CW, Li L, Wang BL, Li QY, Chung KL, et al. Intrinsic sensing properties of chrysotile fiber reinforced piezoelectric cement-based composites. Sensors. 2018;18(9):2999–3008.
[4] Al-Dahawi A, Ozturk O, Emami F, Yildirim G, Sahmaran M. Effect of mixing methods on the electrical properties of cementitious composites incorporating different carbon-based materials. Constr Build Mater. 2016;104:160–8.

[5] Sanchez J, Andrade C, Torres J, Rebolledo N, Fullea J. Determination of reinforced concrete durability with on-site resistivity measurements. Mater Struct. 2017;50:884–7.
[6] Danoglidis PA, Konsta-Gdoutos MS, Shah SP. Relationship between the carbon nanotube dispersion state, electrochemical impedance and capacitance and mechanical properties of percolative nanoreinforced OPC mortars. Carbon. 2019;145:218–28.
[7] Reiterman R, Holcapek O, Zobal O, Keppert M. Freeze–thaw resistance of cement screed with various supplementary cementitious materials. Rev Adv Mater Sci. 2019;58:66–74.
[8] Li H, Xiao HG, Ou JP. Effect of compressive strain on electrical resistivity of carbon black-filled cement-based composites. Cem Concr Compos. 2006;28:824–8.
[9] Luo JL, Zhang CW, Duan ZD, Wang BL, Li QY, Chung KL, et al. Influences of multi-walled carbon nanotube (MCNT) fraction, moisture, stress/strain level on the electrical properties of MCNT cement-based composites. Sens Actuat A Phys. 2018;280:413–21.
[10] Ventrapragada LK, Creager SE, Rao AM, Podila R. Carbon nanotubes coated paper as current collectors for secondary Li-ion batteries. Nanotechnol Rev. 2019;8:18–23.
[11] Power AC, Gorey B, Chandra S, Chapman J. Carbon nanomaterials and their application to electrochemical sensors: a review. Nanotechnol Rev. 2018;7:19–41.
[12] Lin XT, Han Q, Huang JZ. Effect of defects on the motion of carbon nanotube thermal actuator. Nanotechnol Rev. 2019;8:79–89.
[13] Zhan MM, Pan GH, Zhou FF, Mi RJ, Shah SP. *In situ*-grown carbon nanotubes enhanced cement-based materials with multifunctionality. Cem Concr Compos. 2020;108:103518–28.
[14] Han BG, Sun SW, Ding SQ, Yu X, Ou JP. Review of nanocarbon-engineered multifunctional cementitious composites. Compos Part A App Sci Manufact. 2015;70:69–81.
[15] Han BG, Yu X, Kwon E. A self-sensing carbon nanotube/cement composite for traffic monitoring. Nanotechnology. 2009;20:445501–10.
[16] Han BG, Zhang K, Burnham T, Kwon E, Yu X. Integration and road tests of a self-sensing CNT concrete pavement system for traffic detection. Smart Mater Struct. 2013;22:15020–7.
[17] Dong WK, Li WG, Wang KJ, Han BG, Sheng DC, Shah SP. Investigation on physicochemical and piezoresistive properties of smart MWCNT/cementitious composite exposed to elevated temperatures. Cem Concr Compos. 2020;112:103675–87.
[18] Li GY, Wang PM, Zhao XH. Pressure-sensitive properties and microstructure of carbon nanotube reinforced cement composites. Cem Concr Compos. 2007;29:377–82.
[19] D'Alessandro A, Rallini M, Ubertini F, Materazzi AL, Kenny JM. Investigations on scalable fabrication procedures for self-sensing carbon nanotube cement-matrix composites for SHM applications. Cem Concr Compos. 2016;65:200–13.
[20] Luo JL, Duan ZD, Li H. The influence of surfactants on the processing of multi-walled carbon nanotubes in reinforced cement matrix composites. Phys Status Solidi A. 2009;206(12):2783–90.
[21] Luo JL, Chung KL, Li QY, Chen SJ, Li L, Hou DS, et al. Piezoresistive properties of cement composites reinforced by functionalized carbon nanotubes using photo-assisted Fenton. Smart Mater Struct. 2017;26:35025–34.
[22] Isfahani FT, Li WW, Redaelli E. Dispersion of multi-walled carbon nanotubes and its effects on the properties of cement composites. Cem Concr Compos. 2016;74:154–63.
[23] Collins F, Lambert J, Duan WH. The influences of admixtures on the dispersion, workability, and strength of carbon nanotube–OPC paste mixtures. Cem Concr Compos. 2012;34(2):201–7.
[24] Hu T, Jing HW, Li L, Yin Q, Shi XS, Zhao ZL. Humic acid assisted stabilization of dispersed single-walled carbon nanotubes in cementitious composites. Nanotechnol Rev. 2019;8:513–22.
[25] Gao Y, Jing HW, Zhou ZF. Fractal analysis of pore structures in graphene oxide-carbon nanotube based cementitious pastes under different ultrasonication. Nanotechnol Rev. 2019;8:107–15.
[26] Gao Y, Jing HW, Chen SJ, Du MR, Chen WQ, Duan WH. Influence of ultrasonication on the dispersion and enhancing effect of graphene oxide–carbon nanotube hybrid nanoreinforcement in cementitious composite. Compos Part B Eng. 2019;164:45–53.
[27] Kim HK, Park IS, Lee HK. Improved piezoresistive sensitivity and stability of CNT/cement mortar composites with low water–binder ratio. Compos Struct. 2014;116:713–9.
[28] Kim HK, Nam IW, Lee HK. Enhanced effect of carbon nanotube on mechanical and electrical properties of cement composites by incorporation of silica fume. Compos Struct. 2014;107:60–9.
[29] Roy S, Petrova RS, Mitra S. Effect of carbon nanotube (CNT) functionalization in epoxy-CNT composites. Nanotechnol Rev. 2018;7(6):475–85.
[30] Hanizam H, Shukor SM, Zaidi OM. Homogenous dispersion and interfacial bonding of carbon nanotube reinforced with aluminum matrix composite: a review. Rev Adv Mater Sci. 2019;58(1):295–303.
[31] Azhari F, Banthia N. Cement-based sensors with carbon fibers and carbon nanotubes for piezoresistive sensing. Cem Concr Compos. 2012;34:866–73.
[32] Panagiota TD, Konstantinos GD, Ilias T, Dimitrios AE, Theodore EM. Carbon nanotubes and nanofibers as strain and damage sensors for smart cement. Mater Today Comm. 2016;8:196–204.
[33] Lee SJ, You I, Zi G, Yoo DY. Experimental investigation of the piezoresistive properties of cement composites with hybrid carbon fibers and nanotubes. Sensors. 2017;7:2516–31.
[34] Han BG, Wang YY, Ding SQ, Yu X, Zhang LQ, Li Z, et al. Self-sensing cementitious composites incorporated with botryoid hybrid nano-carbon materials for smart infrastructures. J Intel Mat Syst Struct. 2017;28:699–727.
[35] Yoo DY, You I, Lee SJ. Electrical and piezoresistive sensing capacities of cement paste with multi-walled carbon nanotubes. Arch Civ Mech Eng. 2018;18:371–84.
[36] Luo JL, Duan ZD, Zhao TJ, Li QY. Hybrid effect of carbon fiber on piezoresistivity of carbon nanotube cement-based composite. Adv Mater Res. 2011;143:639–43.
[37] Metaxa ZS, Seo JWT, Konsta-Gdoutos MS, Hersam MC, Shah SP. Highly concentrated carbon nanotube admixture for nano-fiber reinforced cementitious materials. Cem Concr Compos. 2012;34:612–7.
[38] Song CW, Hong GT, Choi SC. Effect of dispersibility of carbon nanotubes by silica fume on material properties of cement mortars: Hydration, pore structure, mechanical properties,

self-desiccation, and autogenous shrinkage. Constr Build Mater. 2020;265:120318–34.
[39] Stynoski P, Mondal P, Marsh C. Effects of silica additives on fracture properties of carbon nanotube and carbon fiber reinforced Portland cement mortar. Cem Concr Compos. 2015;55:232–40.
[40] Kostrzanowska-Siedlarz A. Statistical methods for determining rheological parameters of mortars modified with multi-walled carbon nanotubes. Constr Build Mater. 2020;253:119213–24.
[41] Geraldo V, de Oliverira S, da Silva EE, de Oliveria CAS, de Cunha RMA, de Oliverira RFP, et al. Synthesis of carbon nanotubes on sand grains for mortar reinforcement. Constr Build Mater. 2020;252:119044–51.
[42] Metaxa ZS, Pasiou ED, Dakanali I, Stavrakas I, Triantis D, Kourkoulis SK. Carbon nanotube reinforced mortar as a sensor to monitor the structural integrity of restored marble epistyles under shear. Proced Struct Integr. 2016;2:2833–40.
[43] Hawreen A, Bogas JA, Dias APS. On the mechanical and shrinkage behavior of cement mortars reinforced with carbon nanotubes. Constr Build Mater. 2018;168:459–70.
[44] Kaur R, Kothiyal NC, Arora H. Studies on combined effect of superplasticizer modified graphene oxide and carbon nanotubes on the physico-mechanical strength and electrical resistivity of fly ash blended cement mortar. J Build Eng. 2020;30:101304–11.
[45] Wansom S, Kidner NJ, Woo LY, Mason TO. AC-impedance response of multi-walled carbon nanotube/cement composites. Cem Concr Compos. 2006;26:509–19.
[46] Luo JL, Chen SC, Li QY, Liu C, Gao S, Zhang JG, et al. Influence of graphene oxide on mechanical properties, fracture toughness, and microhardness of recycled concrete. Nanomaterials. 2019;9:325–38.
[47] Wang YL, Wang YS, Wan BL, Han BG, Cai GH, Li ZZ. Properties and mechanisms of self-sensing carbon nanofibers/epoxy composites for structural health monitoring. Compos Struct. 2018;200:669–78.